Paper No.
02-1719

Corrosion Prediction with 3-D Model Utilizing Meteorological Data and Properties of Site-extracted Rebar and Concrete

Gang Li
University of Saskatchewan
57 Campus Drive
Saskatoon, SK, S7N 5A9
Canada

Moh Boulfiza
University of Saskatchewan
57 Campus Drive
Saskatoon, SK, S7N 5A9
Canada

Richard Evitts
University of Saskatchewan
57 Campus Drive
Saskatoon, SK, S7N 5A9
Canada

ABSTRACT

In this research, the corrosion of rebar in an existing arch bridge section was modelled. Historical environmental and exposure conditions were used to determine the moisture content, chloride ion concentration and carbonation in the concrete. Then the corrosion rate was calculated by correlating measured pore solution composition of cored concrete with electrochemical corrosion measurements of extracted rebar.

The simulation results for the past 100 years of service correlate very nicely with the current condition of the arch, where the greatest amount of corrosion was predicted to occur on the upper layer of longitudinal rebars in the vicinity of the most exposed side of the arch, and the highest corrosion damage (0.1—0.2 mm thickness loss) was found on that rebar near the columns. The rebars in vertical columns and arch sheltered areas have an insignificant corrosion damage due to limited exposure to moisture. It is concluded that a combination of carbonation and chloride ingress accelerates corrosion rates of the rebar. Ineffective sheltering from the rain or more rain water retention on the arch facilitates this penetration and leads to higher corrosion rates.

Key words: 3-D model, simulation, concrete, corrosion, bridge

INTRODUCTION

Civil infrastructures, such as bridges, may develop varying microenvironments around the reinforcing rebars in the service conditions. Exposed weather conditions, chloride from different sources, carbonation of concrete, and geometry of the structural member all affect the concrete condition, and

hence the corrosion rate of embedded steel rebars. Therefore, it is necessary to consider the local exposure condition of an infrastructure when predicting its corrosion rate.

This model simulates a half-arch section using the 3-D geometry of Arch C of the University Bridge in Saskatoon, SK, Canada. In this model, the main corrosion-determining factors such as moisture content, chloride content, and carbonation were modelled incorporating historical environmental and exposure conditions. These factors were coupled in the model because the moisture content at every point within the concrete of the bridge arch and its fluctuations over time have a direct impact on the transport of the chloride ion and on the evolution of the carbonation front. Given the chloride content and carbonation front, the corrosion rate was estimated using relations from the corrosion rate measurement of the extracted rebars in simulated pore solutions.

MODEL DEVELOPMENT

The 3-D model of the arch component defines the geometry of the domain, where the governing equations that describe the transport of water, chloride ion, and carbon dioxide gas were applied. Boundary conditions were also selected to properly reproduce the exposure environment of the arch. In addition, the corrosion rate of rebar in concrete was correlated from the corrosion rate of the in-situ extracted rebar in a synthetic solution mimicking the pore solution from the in-situ extracted concrete cores.

Governing Equations

Water Flow in Concrete

In many practical conditions, a porous medium like concrete is not fully saturated. The degree of saturation depends on the surrounding environmental moisture conditions. When concrete is not fully saturated, a negative capillary pressure develops and facilitates the absorption of water and this pressure is the driving force of water flow within concrete. Under such conditions the permeability becomes dependent on the water content. Darcy's law has been extended to describe water flow for this kind of problem in unsaturated porous media. One of the earliest and most widely used models for water flow in unsaturated porous media is known as Richard's equation. When coupled with the mass balance equation for an unsaturated porous medium, the governing equation becomes

$$C\frac{\partial H_p}{\partial t} = \nabla \cdot \left[K_s k_r \nabla (H_p + Z)\right] \tag{1}$$

where, H_p [m] is pressure head, z [m] is elevation, t [s] is time, K_s [m/s] is hydraulic conductivity of concrete at full saturation and K_r is relative permeability, defined as the ratio between the hydraulic conductivity at volumetric water content θ, $K(\theta \leq \theta_s)$ to $K(\theta = \theta_s)$, where θ_s [-] is saturated water content or the total connected porosity, C [1/m] is defined as change in storage due to change in pressure head.

$$C = \frac{\partial \theta}{\partial H_p} \tag{2}$$

A constitutive relationship or model that has been shown to work with concrete is given is van Genuchten- Mualem model,[1,2] given by Equations (3-6):[3,4]

$$C = S_e \cdot S_s + \frac{\alpha m}{1 - m}(\theta_s - \theta_r)S_e^{\frac{1}{m}}Se^l\left(1 - S_e^{\frac{1}{m}}\right)^m \tag{3}$$

$$k_r = S_e^l \left(1 - \left(1 - S_e^{\frac{1}{m}}\right)^m\right)^2 \tag{4}$$

$$S_e = \begin{cases} \left[1 + |\alpha H_p|^n\right]^{-m}, & H_p < 0 \\ 1, & H_p \geq 0 \end{cases} \tag{5}$$

$$S_e = \frac{\theta - \theta_r}{\theta_s - \theta_r} \tag{6}$$

where, k_r[-] is relative permeability, S_e[-] is effective saturation, θ_s [-] is saturated water content, θ_r[-] is residual water content, S_s [1/m] is storage coefficient. l [-], m [-], n [-], and α [1/m] are empirical parameters ($m = 1 - 1/n$). These empirical parameters were estimated from a water retention test specifically for the extracted concrete from the arch.

These empirical parameters for the site-extracted concrete were determined by a water retention test conducted in the environmental lab of the University of Saskatchewan. This test examined how the degree of saturation depends on the surrounding environmental moisture conditions. The extracted concrete from the University bridge arch were sliced and put in humidity chambers with relative humidity (RH) ranging from 14.5%-100% to reach the equilibrium with the surrounding water vapour. The relationship between pressure head and RH can be derived from the Kelvin and Young-Laplace equation:

$$\ln(RH) = \left(\frac{H_p V_m \rho g}{RT}\right) \tag{7}$$

where RH [-] is relative humidity, H_p [m] is pressure head, V_m [$m^3 \cdot mol^{-1}$] is the molar volume of liquid, ρ [$kg \cdot m^{-3}$] is density of water, g [$m \cdot s^{-2}$] is gravitational accretion rate, R [$J \cdot mol^{-1} \cdot K^{-1}$] is gas constant, and T [K] is temperature.

The RH were then converted into the pressure head(H_p) in these sliced concrete samples in each humidity chamber. The effective saturation (S_e) of each sample was determined by measuring the sample weight change at the equilibrium state in each humidity chamber with respect to its vacuumed-water-saturated state. The empirical parameters α=0.0018 [1/m], and n=1.7 were then determined by curve fitting the H_p-S_e data with Equation (5), as shown in Figure 1.
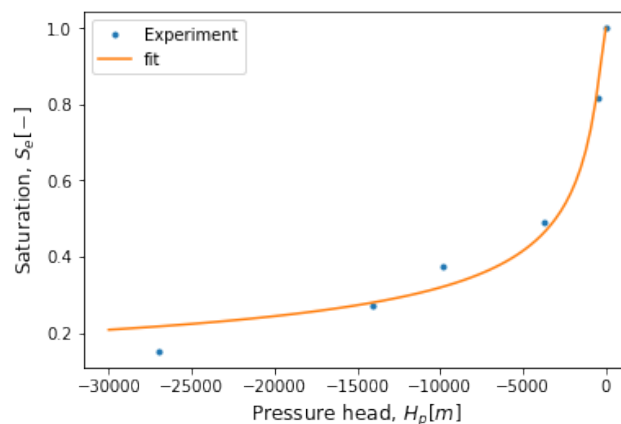

Figure 1: Saturation as a function of pressure head.

<u>Chloride ion transport and carbonation</u>

The transport of salts in concrete is governed by the diffusion-advection equation, whereby:

$$\frac{\partial(\theta c)}{\partial t} = -\nabla \cdot \mathbf{J} \tag{8}$$

$$\mathbf{J} = -D_{eff}\theta\frac{\partial c}{\partial z} + \mathbf{u}c \tag{9}$$

$$D_{eff} = D_s \cdot \Phi(S_e) \tag{10}$$

where $\mathbf{J}$ $[kg \cdot m^2 s^{-1}]$ is the total volume-averaged mass flux of solute in concrete, $\mathbf{u}$ $[m \cdot s^{-1}]$ is the Darcy's velocity, c $[kg \cdot m^{-3}]$ is the liquid phase-averaged solute concentration, D_{eff} $[m^2 \cdot s^{-1}]$ effective diffusivity, D_s is effective diffusivity under fully saturated conditions, $\Phi(S_e)$ is a reduction function that accounts for discontinuity in the liquid phase, determined by experiment.

Carbonation is modelled as a gas diffusion problem. The calculated concentration of carbon dioxide is calibrated to pH in a carbonated synthetic pore solution.

$$\frac{\partial(\theta_s S_g C_{co_2})}{\partial t} = \nabla \cdot \left[D_{co_2} \cdot \nabla C_{co_2} \right] \tag{11}$$

where, S_g is the volume fraction of gas to the total porosity, D_{co_2} is the effective diffusion coefficient of CO_2 in concrete, which is also a function of concrete saturation level.

Boundary Conditions

<u>Boundary conditions for water flow in concrete</u>

Pressure head, a function of temperature and relative humidity (obtained from RH though Equation 7), was chosen as the boundary conditions, which represents the moisture environments the concrete arches were exposed to, and fundamentally affects the transport properties of arch concrete. The raw weather data (temperature, RH, Precipitation) were collected from two weather stations: SASKATOON DIEFENBAKER INT'L A, and SASKATOON RCS. All raw hourly data were smoothed through an in-house moving average filter.
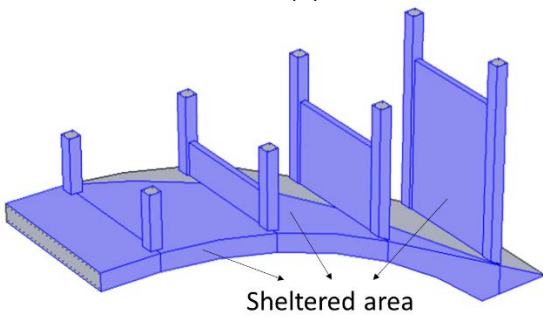
- Sheltered area
  Hourly and daily data from year 2007–2014, and normalized monthly data from year 1981 to year 2010 were used to determine the averaged boundary conditions for the sheltered portion of the arch; the averaged value of pressure head was determined through a non-linear regression analysis (Figure 2ab). The averaged boundary conditions were applied to all the columns, curtain walls, arch soffit, and selected arch top area that is protected by spandrel walls and deck (Figure 2c).
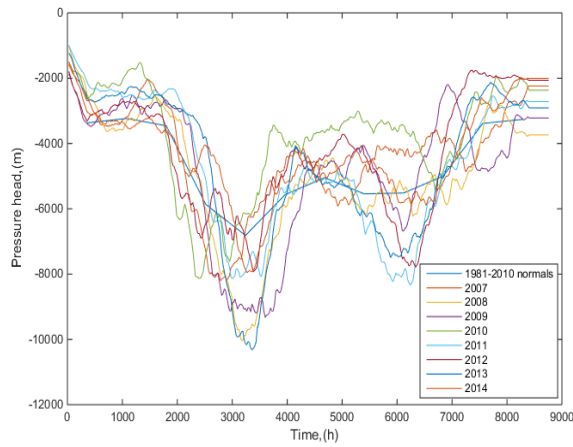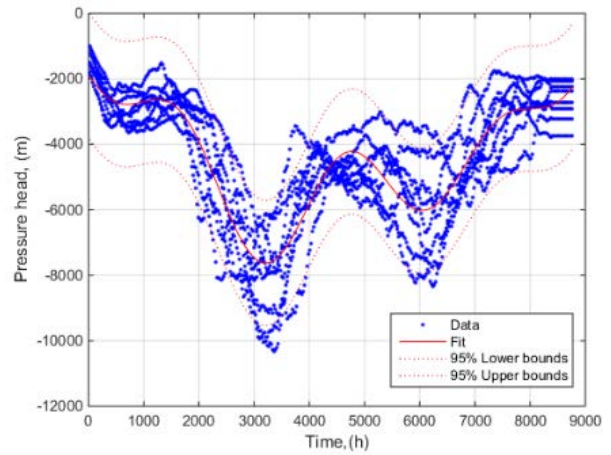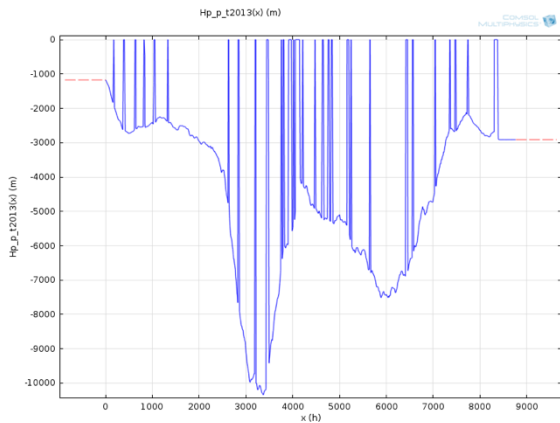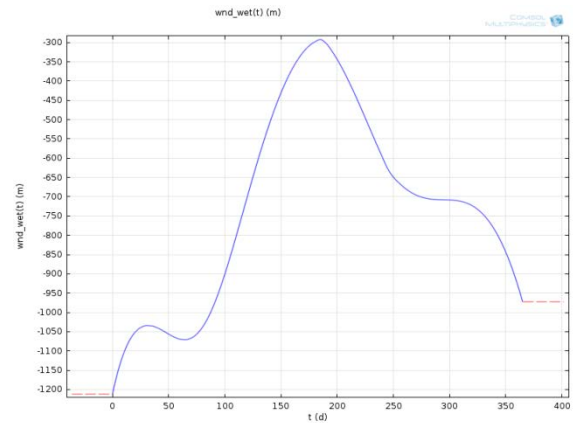
Figure 2: Moisture boundary conditions for the sheltered portion of an arch: (a) Raw data of pressure head obtained from weather station; (b) averaged data fitted from the raw data; (c) location of sheltered area (in blue).
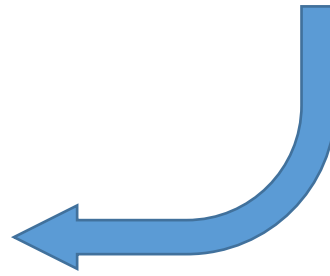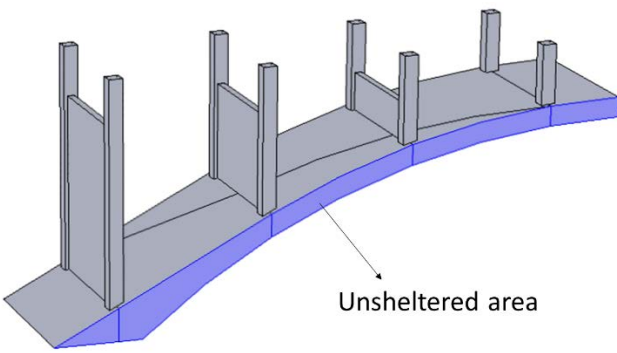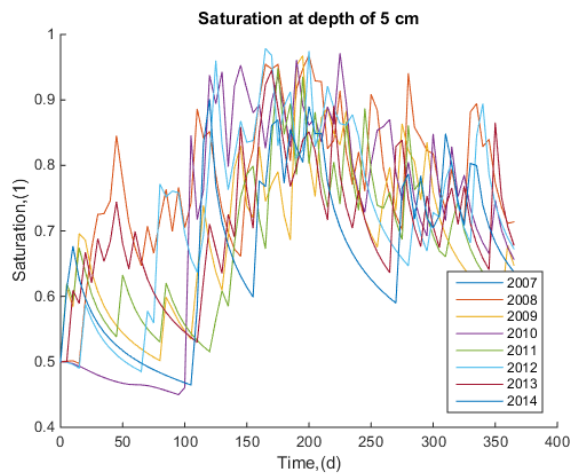
- Unsheltered areas

The unsheltered areas are exposed to both air moisture and rain. Figure 3a shows the unsheltered boundary condition for year 2013, where the vertical lines switch pressure head instantly to 0 representing soaking wet on the concrete surface. An equivalent smooth boundary condition (Figure 3b) was developed to reduce computational complexity. This equivalent curve was calibrated for the saturation fluctuation at depth of 5 cm, 10 cm, and 15 cm for year 2007–2014 in a 2-D model (Figure 4).
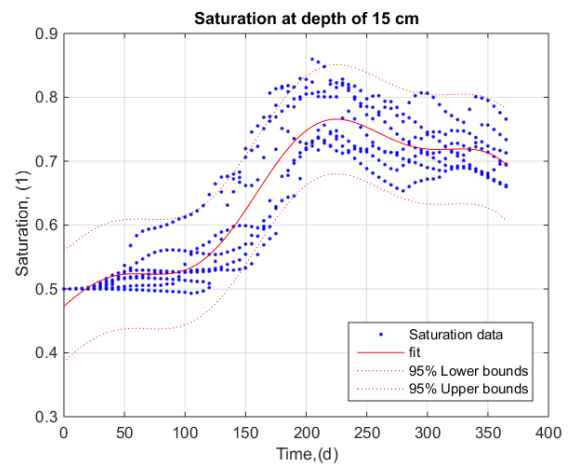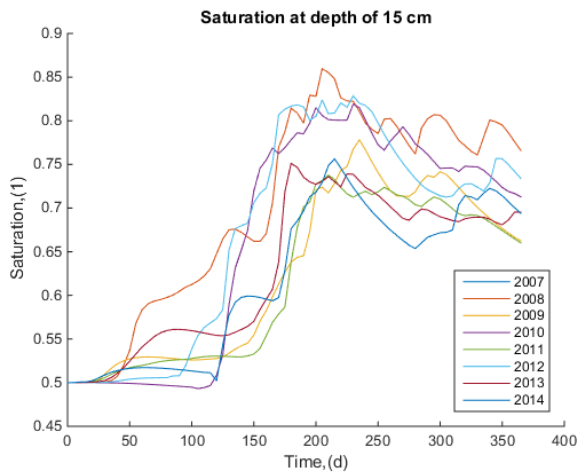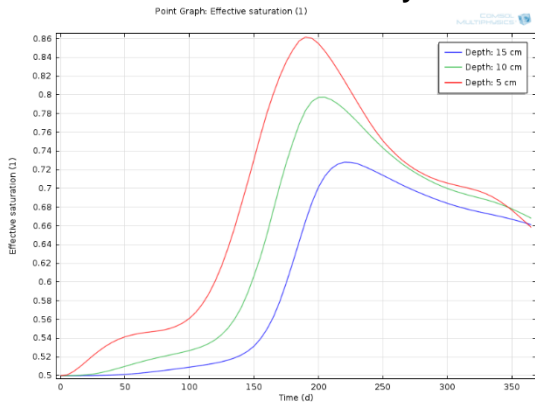
(c)

Figure 3: Moisture boundary conditions for the unsheltered portion of the arch (eg, Year 2013, after calibration): (a) Raw data of pressure head obtained from weather station; (b) the equivalent smooth boundary condition; (c) location of unsheltered area (in blue).
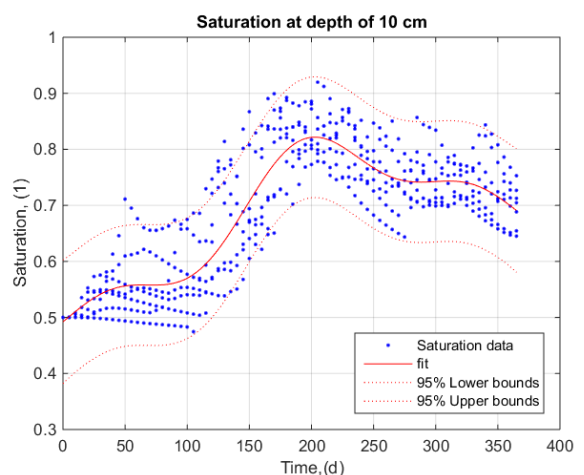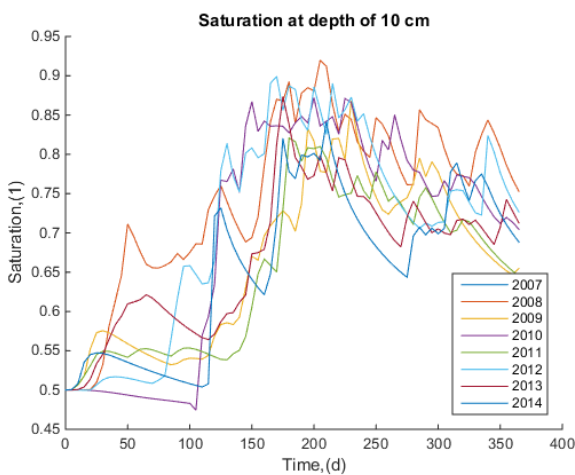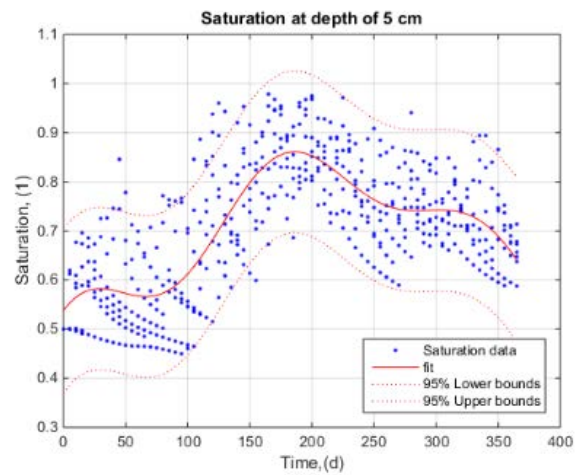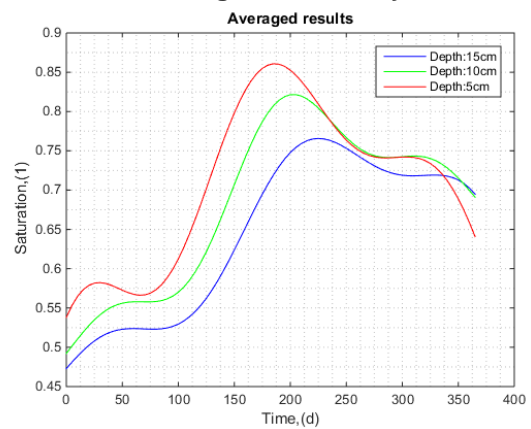
Figure 4: Calibration of the smoothed boundary conditions for the unsheltered portion of an arch.

- Partially sheltered area

These areas are also exposed to a varying combination of air moisture and rain (Figure 5). Three 2-D linear ramp functions were used to describe the varying combinations, such that the weights of sheltered condition and unsheltered condition were 0 and 1 on the edge of the arch and 1 and 0 on the diagonal line on the arch.
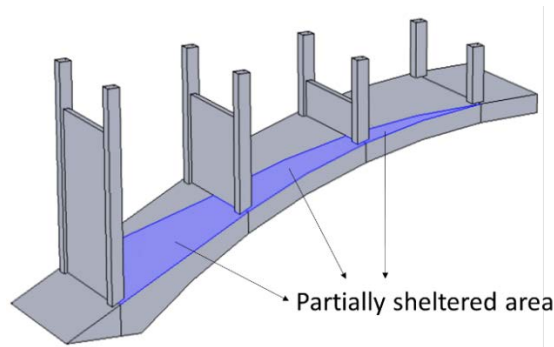

Figure 5: Moisture boundary conditions for partially sheltered area.

<u>Boundary conditions for chloride ion transport</u>

Boundary conditions for chloride ion transport consisted of two conditions: "concentration" and "insulation". Under the "concentration" condition, the concrete surface was subject to 3% NaCl solution, while in "insulation" there was a zero flux of chloride ion and existing chloride ions are free to transport according to concentration gradients and water flow within concrete. The "concentration" boundary condition was implemented for 90 days of simulated annual time during May 15 to July 15 due to high volume of precipitation and accumulated deicing salts from the winter season. For the rest of the time, "insulation" was implemented. These conditions were applied to the completely or partially sheltered regions as illustrated in Figure 6.
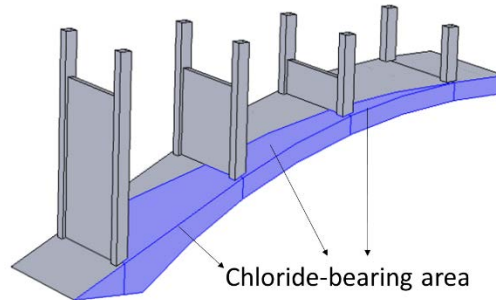

Figure 6: Boundary condition for chloride ion transport.

<u>Boundary conditions for CO_2 transport</u>

For the CO_2 boundary conditions, a constant 0.03% CO_2 concentration was applied to all exposed arch areas including curtain walls, columns, arch top and soffit, as presented in Figure 7.
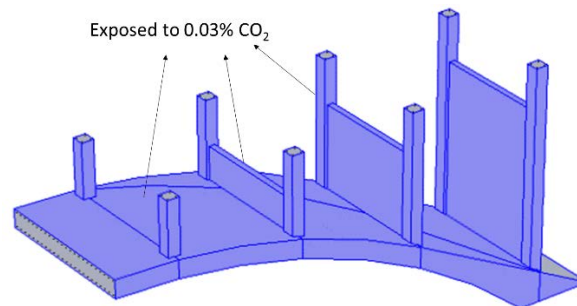

Figure 7: Carbonation boundary conditions.

Corrosion rate correlation

In this large scale 3-D model, the corrosion rate of rebar in concrete is correlated to the chloride concentration, pH, and saturation in concrete in rebar locations. The corrosion rate of the rebar was correlated to corrosion rates in a simulated pore solution which was formulated based on the extracted pore solution composition from the cored concrete sample from the bridge by the centrifuge technique. The corrosion rate was measured by potentiodynamic scans of rebars in the simulated pore solution with various levels of chloride concentration, and pH levels in a previous work.[5] The interpolated results is shown in Figure 8. The effect of saturation on rebar corrosion rate in concrete was accounted by a reduction factor, which was based on the measurement of reinforced concrete corrosion rate at different saturation levels, known as Tuutti's curve[6].
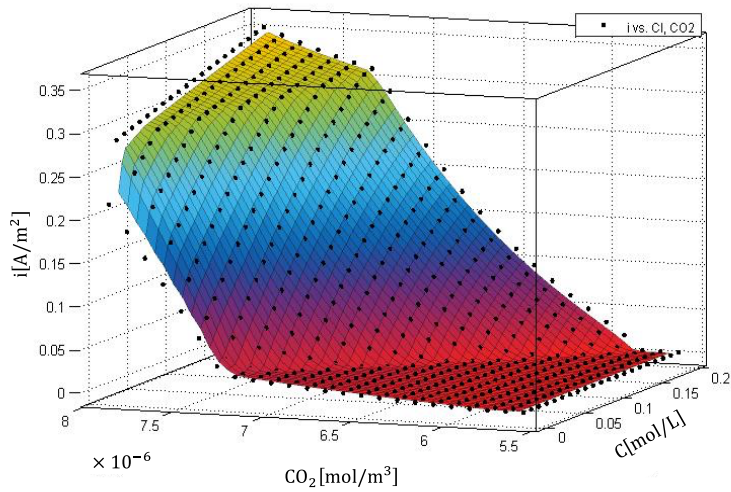
Figure 8: Corrosion current density, i (A/m^2), versus chloride concentration, Cl (M), and calibrated carbon dioxide concentration, CO$_2$ (mol/m^3), where carbon dioxide concentrations are estimated and empirically calibrated to pH values found in concrete.
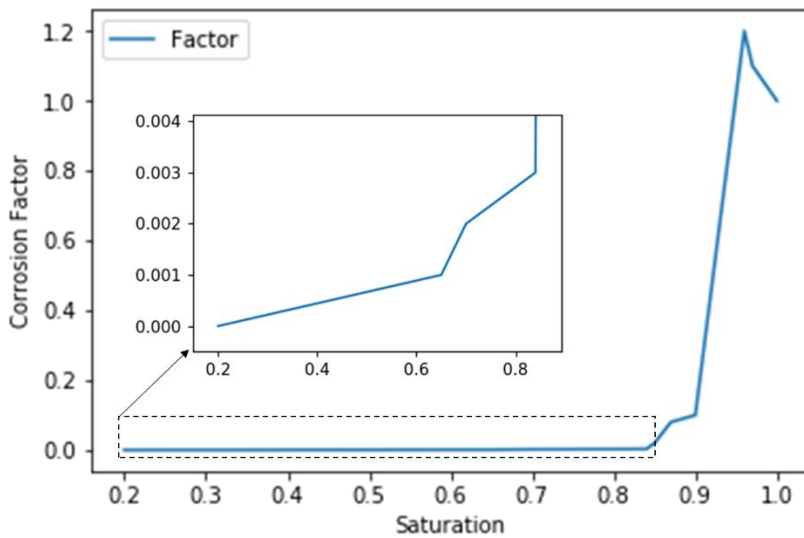

Figure 9: Reinforced concrete corrosion rate factor relative to saturated condition, adapted from Tuutti's curve[6].

SIMULATION RESULTS

For the simulated case of 100 years of exposure, the predicted distribution of pH and concentration of chlorides are plotted in Figure 10 and Figure 11, respectively. As the carbonation and chloride ion ingress proceeded through the concrete cover, the once passivated rebar became active and thus has a higher corrosion rate occurred. The corrosion loss in thickness was calculated by the integration of corrosion rate over time. The results of corrosion loss in thickness on the rebar after 100 years of exposure are plotted in Figure 12 and prediction of additional corrosion between 101 years and 150 years of service is plotted in Figure 13.
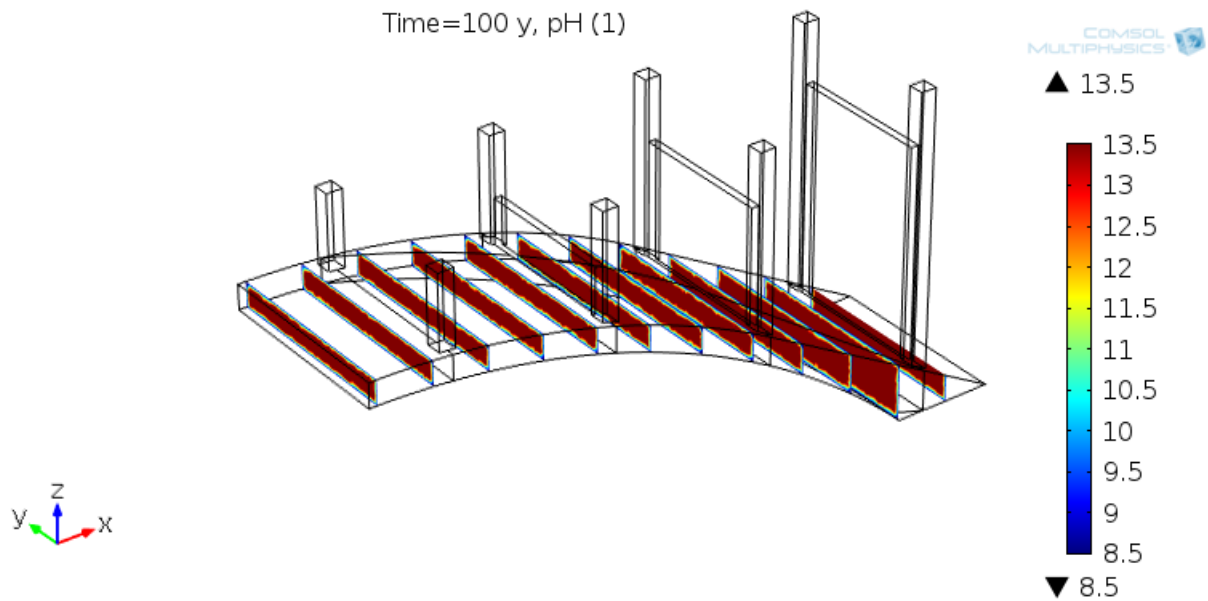
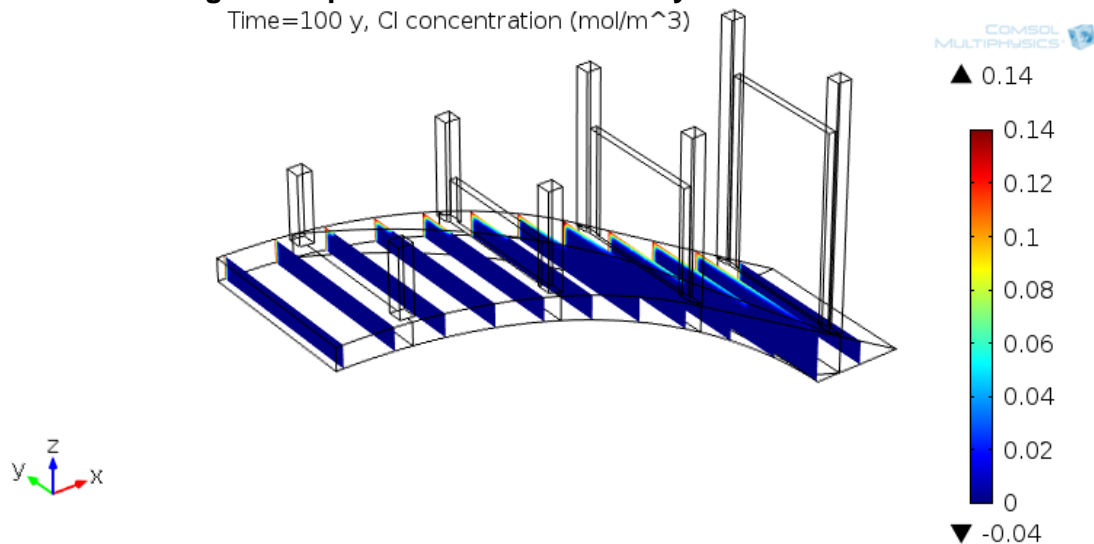**Figure 10: pH distribution after 100 years carbonation.**

Figure 11: Chloride concentration distribution after 100 years of exposure.

As shown in Figure 12(a) where the corrosion thickness lose is plotted in log scale, the majority of corrosion is predicted to occur on the upper layer of longitudinal rebars that is close to the most exposed arch edge where the highest localized corrosion (0.2 mm and 0.1 mm loss in thickness) is predicted on that layer of rebars near the columns. High corrosion losses are mainly found on the two longitudinal rebars near the most exposed edges, and occasionally on the upper layer rebars in the partially sheltered area near the curtain walls.

Upper layers of rebar in the partially sheltered area have both carbonation and chloride exposure to a lesser extent than the arch edge rebars, and thus have a moderate predicted corrosion loss. In the sheltered area of the arch, a low corrosion rate shows that without exposure to direct rain and runoff water, chloride transport has limited effect on the corrosion. The vertical column rebars have an insignificant corrosion loss due to limited exposure to moisture, even though these rebars have the least concrete cover thickness and the carbonation induced pH drop would increase the overall corrosion rate. If this part of the bridge remains untreated for another 50 years, corrosion loss is predicted to increase significantly due to a deeper carbonation and more accumulation of chloride ions.

As shown Figure 13, the maximum additional loss in thickness is slightly larger than that in the previous 100 years all together. The severity of corrosion in partially saturated area approaches the condition in the most exposed area.
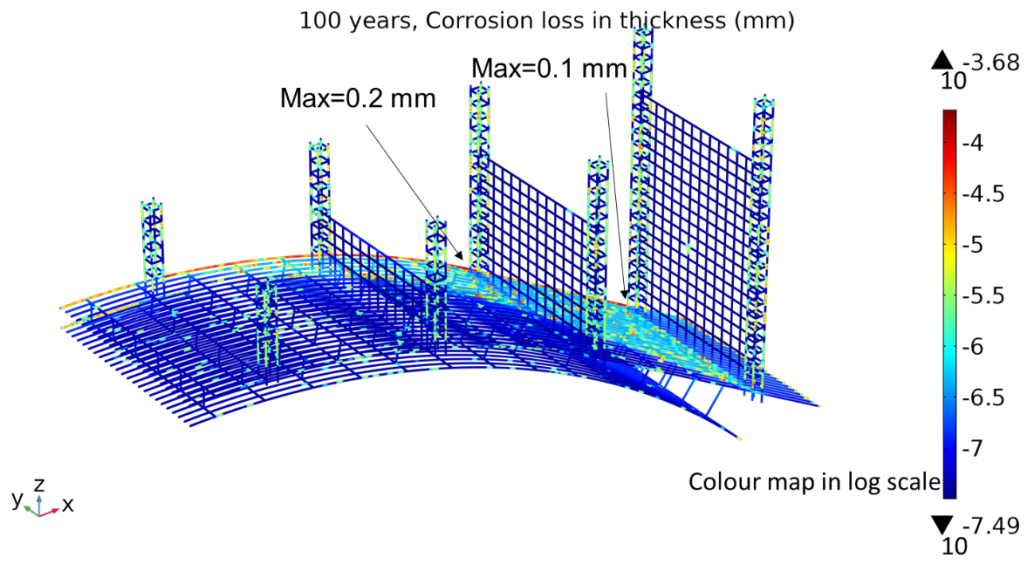
(a)
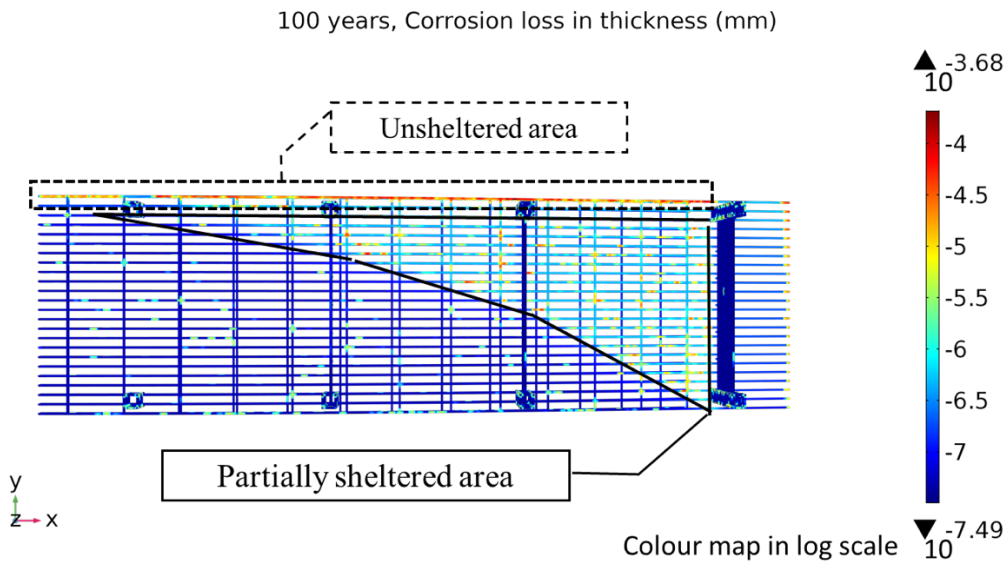
(b)

Figure 12: Corrosion loss in thickness after 100 years of exposure, plot in log scale (a) 3D view (b) XY view.
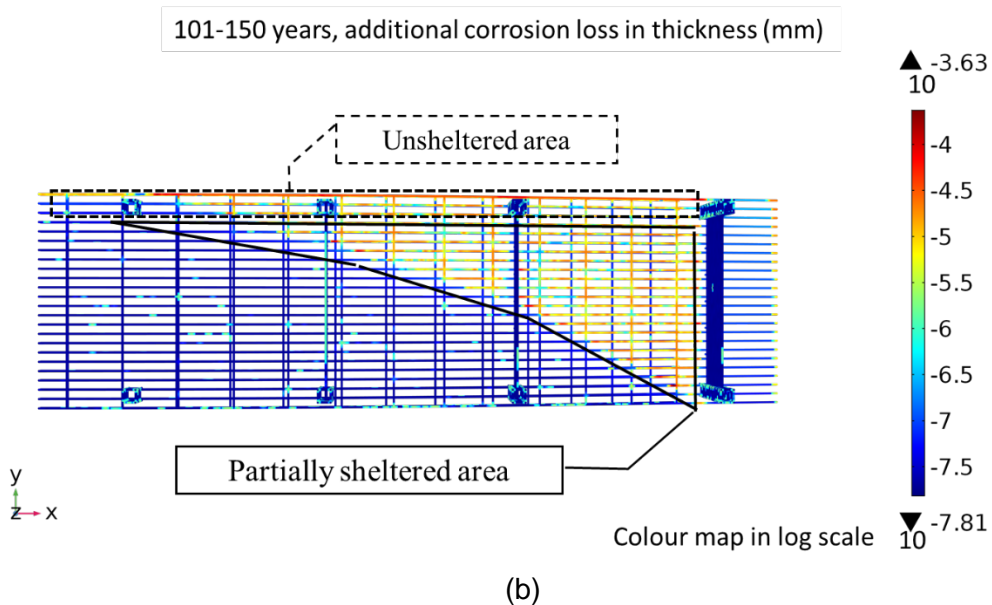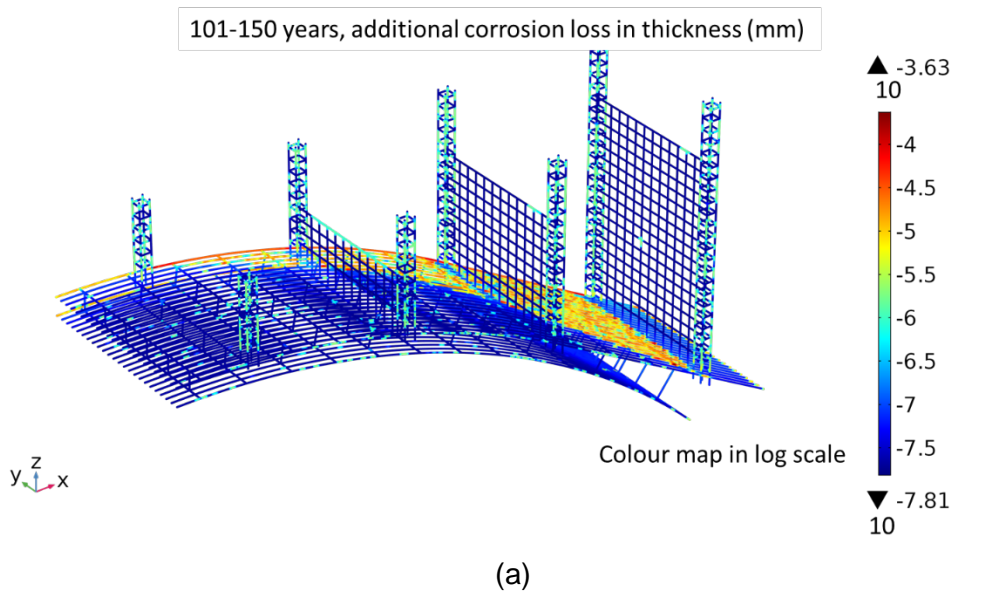
(a)

(b)

Figure 13: Additional corrosion loss from101 years-150 years of exposure, plot in log scale (a)3D view (b) XY view.

CONCLUSIONS

The microenvironment including chloride content, pH, and saturation may not be uniform across whole reinforced concrete structure, due to different exposure conditions. In the simulated University Bridge arch component, a combination of carbonation and chloride ingress accelerates corrosion rates of rebar. Ineffective sheltering from the rain or more rain water retention on the arch facilitates this penetration and leads to higher corrosion rates.

ACKNOWLEDGEMENTS

REFERENCES

1.   A. Kumar. "Water Flow and Transport of Chloride in Unsaturated Concrete" (Master's thesis. University of Saskatchewan, 2010).

2.   G. Li, "Effect of Cracks on the Transport Characteristics of Cracked Concrete" (Master's thesis, University of Saskatchewan, 2014).

3.   Y. Mualem, "A new model for predicting the hydraulic conductivity of unsaturated porous media." *Water resources research* 12, 3 (1976): p. 513-522.

4.   M. T. Van Genuchten, A closed-form equation for predicting the hydraulic conductivity of unsaturated soils 1. *Soil science society of America journal* 44, 5 (1980): p. 892-898.

5. G. Kennell, J. ZACARUK, G. Li, & M. Boulfiza, The University Bridge Arch Assessment-A New Approach. 2015 Transportation Association of Canada (TAC) Conference & Exhibition, (Charlottetown, PEI, Canada 2015) p. 7-8.

6. K. Tuutti, Corrosion of Steel in Concrete, Swedish Cement and Concrete Research Institute, Stockholm, Sweden, January 1982. p. 85.